Negative Curvature Surfaces in Chemical Structures

R. B. King

Department of Chemistry, University of Georgia, Athens, Georgia 30602

Received August 30, 1997

Regular tessellations of polygons are not only possible for flat planes (e.g., the {4,4}, {6,3}, and {3,6} tessellations) and the sphere (e.g., the {3,3}, {4,3}, {3,4}, {5,3}, and {3,5} tessellations corresponding to the regular polyhedra), but also for surfaces of negative Gaussian curvature (i.e., hyperbolic planes), of which the {7,3}, {8,3}, and {6,4} tessellations are of greatest actual or potential chemical interest. However, it is not possible to construct an infinite surface with a *constant* negative Gaussian curvature to accommodate such tessellations because the pseudosphere, the negative curvature "analogue" of the sphere, has an inconvenient cuspidal singularity that prevents it from being used to describe periodic chemical structures. However, patches of *varying* negative curvature and constant zero mean curvature can be smoothly joined to give various infinite periodic minimal surfaces (IPMSs), which have zero mean curvature and are periodic in all three directions. The unit cells of the simplest IPMSs have genus 3 so that the unit cells of the {7,3}, {8,3}, and {6,4} tessellations on such IPMSs can be shown by a generalization of Euler's theorem to contain 24 heptagons, 12 octagons, and 8 hexagons, respectively. The {7,3} and {8,3} tessellations on suitable IPMSs can be used to derive possible structures of low-density polymeric carbon allotropes. Crystallography in the hyperbolic plane based on the {6,4} tessellation embedded in similar IPMSs has been used by Sadoc and Charvolin to model the properties of bilayers in liquid crystal and micellar structures.

1. INTRODUCTION

A number of important features of chemical structures can be described by polyhedra, where a polyhedron can be regarded as a polygonal net embedded in the surface of a sphere or other positive curvature surface topologically homeomorphic to the sphere or a fragment thereof. For example, polyhedra can appear as coordination polyhedra in which the vertices represent ligands surrounding a central atom that is often, but not always, a metal, and cluster polyhedra in which the vertexes represent multivalent atoms and the edges represent bonding distances. In general, a single polyhedron describes a finite structure although infinite polymeric structures can be generated by linking polyhedra in various ways.

A question of mathematical interest that is also relevant to a few areas of chemistry relates to the properties of polygonal nets embedded in a surface of negative curvature. Such polygonal nets are relevant to a number of areas of chemistry including possible exotic carbon allotrope structures,[1] the absorption of gases in zeolites,[2,3] phase transitions such as the martensite transformation,[4] and the properties of bilayers in liquid crystal and micellar structures.[5] In this paper, the relevant properties of such negative curvature surfaces, the nature of the embeddings of polyhedral nets in such surfaces, and the application of this area of mathematics to the structures of exotic carbon allotropes as well as bilayers in liquid crystal and micellar structures, is surveyed.

2. REGULAR TESSELLATIONS

2.1. The Nature of Tessellations. Embedding a network of polygons into a surface can be described as a *tiling* or *tessellation* of the surface.[6] In a formal sense, a *tiling* or *tessellation* of a surface is a countable family of closed sets $T = \{T_1,T_2...\}$ that covers the surface without gaps or overlaps. More explicitly, the union of the sets $T_1,T_2...$ (which are known as the *tiles* of T) is the whole surface and the interiors of the sets T_i are pairwise disjoint. In the tessellations of interest in this paper, the tiles are the polygons, which in the case of tessellations corresponding to polyhedra, are the faces of the polyhedra. Tessellations can be described in terms of their *flags*, where a *flag* is a triple (V,E,F) consisting of a vertex V, an edge E, and a face F, which are mutually incident. A tiling T is called *regular* if its symmetry group $G(T)$ is transitive on the flags of T. A regular tessellation consisting of q regular p-gons at each vertex can be described by the so-called Schäfli notation $\{p,q\}$. Tessellations are to be contrasted with packings where a *packing* of a surface is a countable family of closed sets $T = \{T_1,T_2...\}$ that covers the surface without overlaps but that may have gaps. Thus, all tessellations are packings, but not all packings (i.e., those with gaps) are tessellations.

First consider regular tessellations in the Euclidean plane (i.e., a flat surface of zero curvature). In the Euclidean plane, the angle of a regular p-gon, $\{p\}$, is $(1-2/p)\pi$; hence q equal $\{p\}$'s (of any size) will fit together around a common vertex if this angle is equal to $2\pi/q$, leading to the following relationship:

$$(p - 2)(q - 2) = 4 \qquad (1)$$

There are only three integral solutions of eq 1, which lead to the three regular tessellations of the plane {4,4}, {6,3}, and {3,6} depicted in Figure 1. The tessellation {6,3} is familiar in chemistry as the structure of graphite whereas the tessellation {4,4} corresponds to the checkerboard.

Now consider regular tessellations of the sphere that correspond to the regular polyhedra. The angle of a regular *spherical* polygon $\{p\}$ is *greater* than $(1-2/p)\pi$ and gradually

S0095-2338(97)00063-2 CCC: $15.00
Published on Web 02/10/1998

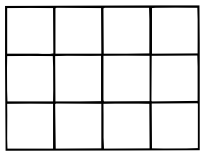

{4,4} ("checkerboard plane")

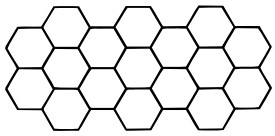

{6,3} ("graphite structure")

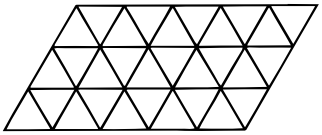

{3,6}

Figure 1. The three regular tessellations of the plane.

increases from this value to π when the circumradius increases from 0 to $\pi/2$. Thus, if

$$(p-2)(q-2) < 4 \qquad (2)$$

then, the size of $\{p\}$ can be adjusted so that its angle is exactly $2\pi/q$; then q such $\{p\}$'s will fit together around a common vertex leading to the regular spherical tessellations $\{2,q\}$, $\{p,2\}$, $\{3,3\}$, $\{3,4\}$, $\{4,3\}$, $\{3,5\}$, and $\{5,3\}$. The tessellation $\{2,q\}$, formed by q lunes (i.e., spherical polygons with two vertexes and two edges) joining two antipodal points, is called the q-gonal *hosohedron*.[7] The tessellation $\{p,2\}$, formed by two p-gons, each covering a hemisphere, is called the p-gonal *dihedron* because it has two faces. The remaining five regular spherical tessellations correspond to the five regular polyhedra (Figure 2 and Table 1).

Finally consider regular tessellations in the hyperbolic plane, where the angle of a regular *hyperbolic* polygon $\{p\}$ is less than $(1-2/p)\pi$ and gradually decreases from this value to zero when the (negative) curvature goes from 0 to $-\infty$. Thus, if

$$(p-2)(q-2) > 4 \qquad (3)$$

then, the size of $\{p\}$ can be adjusted so that its angle is exactly $2\pi/q$; then q such $\{p\}$'s will fit together around a common vertex and further $\{p\}$'s can be added indefinitely. In this manner, we construct a regular *hyperbolic tessellation* $\{p,q\}$, which is an infinite collection of regular p-gons filling the whole hyperbolic plane. There are obviously an infinite number of integral solutions of eq 3 leading to an infinite number of different regular hyperbolic tessellations.

Tetrahedron
{3,3}

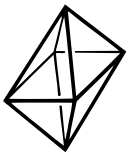

Octahedron
{3,4}

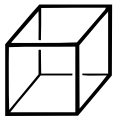

Cube
{4,3}

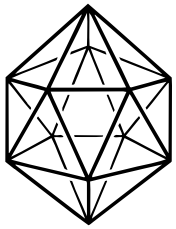

Icosahedron
{3,5}

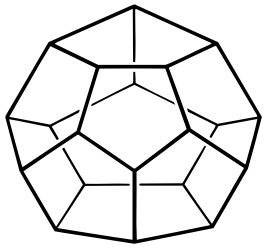

Dodecahedron
{5,3}

Figure 2. The five regular polyhedra as they are derived from regular tessellations of the sphere.

Table 1. Properties of the Regular Polyhedra

polyhedron	face type	vertex degrees	number of edges	number of faces	number of vertices
tetrahedron	triangle	3	6	4	4
octahedron	triangle	4	12	8	6
cube	square	3	12	6	8
icosahedron	triangle	5	30	20	12
dodecahedron	pentagon	3	30	12	20

Let us now consider the hyperbolic tessellations with the lowest values of p and q satisfying eq 3. The tessellation $\{7,3\}$ depicted in Figure 3 was already described in some detail in 19th century work of Klein[8]; this $\{7,3\}$ tesselation and the related $\{8,3\}$ tessellation are the basis of proposed structures for low-density polymeric carbon allotropes.[1] The tessellations $\{5,4\}$ and $\{6,4\}$ are depicted in Figure 4, where the n-gons are divided into $2n$ alternately black and white triangles as is frequently done to indicate their symmetry.[9] The tessellation $\{6,4\}$ has been used by Charvolin and Sadoc[5] in the study of periodic systems of frustrated fluid films and bicontinuous cubic structures in liquid crystals.

2.2 The Relationships of Tessellations to Crystallography. Tessellation of a surface is related to a generalization of the ideas of crystallography, sometimes called *abstract crystallography*. Classical crystallography is concerned with the periodic organization of topologically zero-dimensional objects, such as atoms and molecules, in three-dimensional (3D) space and can relate to the ability of polyhedra to pack in various ways in 3D space. Crystallography is also possible in the plane; the infinite discrete two-dimensional (2D) groups, of which there are 17, arise in practice as the various ways of repeating a flat design, as

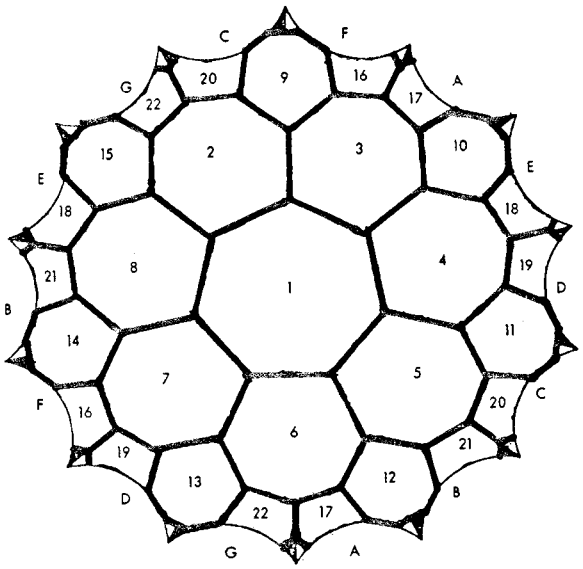

Figure 3. The {7,3} tessellation of the hyperbolic plane.

on wallpaper or a tiled floor. Such 2D crystallography can also relate to the study of periodic organizations of 2D objects such as surfaces or films. Sadoc and Charvolin[10] have also introduced the idea of crystallography in the hyperbolic plane (i.e., a surface with negative curvature), which arises arising from their study of the {6,4} tessellation in connection with their work on liquid crystal and micellar structures.

In considering 2D crystallography there are two ways of looking at the unit cell. For example, in the case of the square lattice of the Euclidean plane corresponding to the {4,4} tessellation (Figure 1), a square cell can be considered either as the fundamental region of the infinite plane or as the surface of the torus obtained by identifying the opposite sides of the square and all four vertices together (Figure 5). The toroidal model effectively makes the infinite plane finite by identifying all points that are equivalent in a translation. Thus, in effect, converting a flat plane to a torus as suggested in Figure 5 substitutes some operations of translations by identifications (e.g., of opposite edges). Furthermore, the toroidal model of a 2D lattice does not require a flat surface but can also be applied to hyperbolic planes. Thus, a polygon with $4g$ vertexes can be considered either as a fundamental region for the translational subgroup or as a toroidal surface obtained by identifying its sides two by two and its vertexes all together analogous to the conversion of a rectangle to a torus depicted in Figure 5. This toroidal model will be useful when considering the genus of infinite periodic minimal surfaces discussed next.

3. NEGATIVE CURVATURE AND INFINITE PERIODIC MINIMAL SURFACES

3.1 Differential Geometry of Surfaces. The methods of differential geometry[11,12] can be used to describe surfaces and their properties. Such methods define a given surface by the following vector equation with the two parameters u and v:

$$r = r(u,v) \tag{4}$$

The basic tangent vectors are then given by:

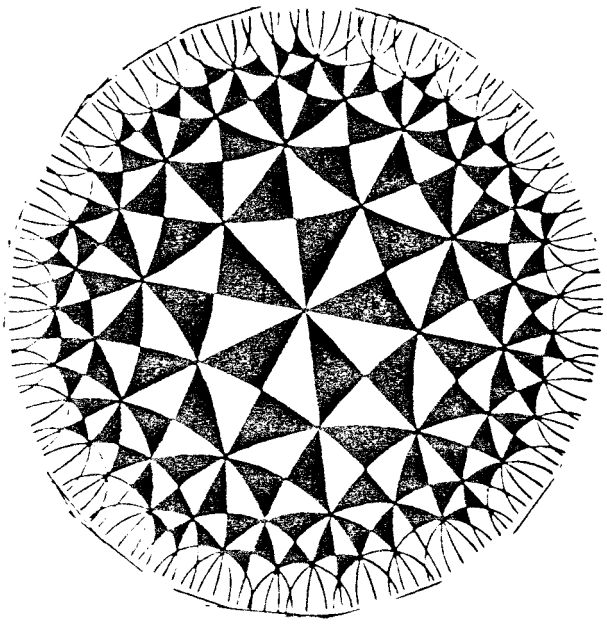

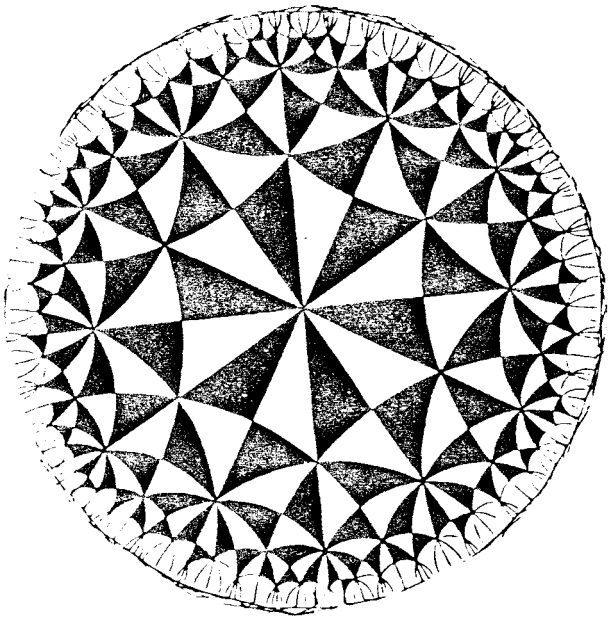

Figure 4. The {5,4} and {6,4} tessellations of the hyperbolic plane as depicted by Coxeter.[9]

$$r_1 = \mathrm{d}r/\mathrm{d}u \text{ and } r_2 = \mathrm{d}r/\mathrm{d}v \tag{5}$$

so that

$$\mathrm{d}r = r_1\mathrm{d}u + r_2\mathrm{d}v \tag{6}$$

The tangent plane to the surface at the point (u,v) is r_1r_2. The so-called *metric tensor* has components defined by:

$$g_{11} = r_1r_1;\ g_{12} = g_{21} = r_1r_2;\ g_2 = r_2r_2 \tag{7}$$

The properties of the surface are then determined from its metric tensor by the use of two fundamental forms. The

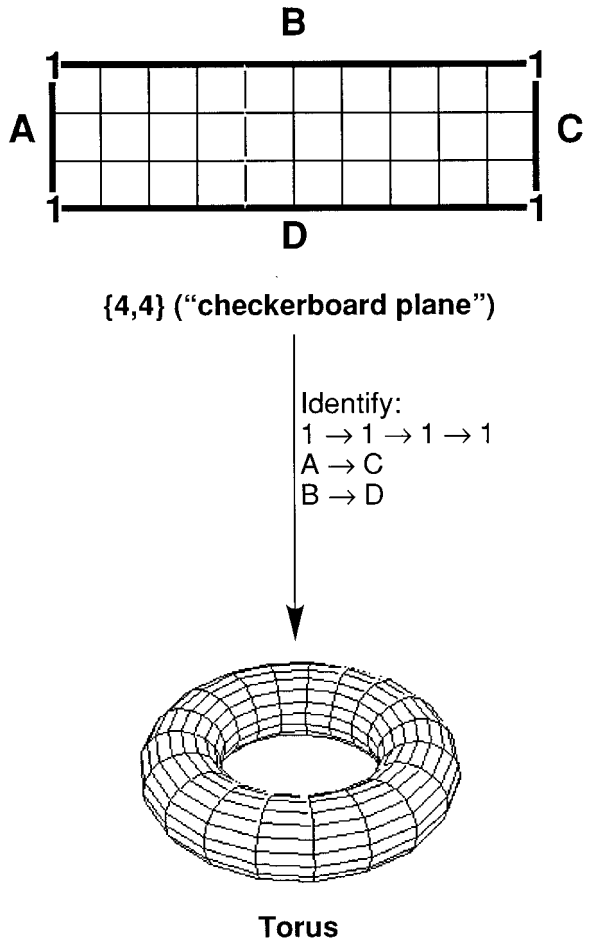

Figure 5. Generation of a torus by identifying all four vertexes (all labeled 1) and both pairs of opposite sides (i.e., A with C and B with D) of a rectangular section of the plane.

first fundamental form for the element of arc d*s* of the surface is given by:

$$ds^2 = dr \cdot dr = g_{11}du^2 + 2g_{12}dudv + g_{22}dv^2 \qquad (8)$$

Now let n be the normal vector to the surface $r = r(u,v)$, let $b_{ij} = r_{ij}n$, and let κ be the normal curvature, different in different directions, of a plane curve formed by a section of the normal plane. The second fundamental form for the element of arc of the surface is given by:

$$\kappa\, ds^2 = b_{11}du^2 + 2b_{12}dudv + b_{22}dv^2 \qquad (9)$$

The first fundamental form (eq 8), which is derived from the tangent vectors, is a measure of the metric of the surface, whereas the second fundamental form (eq 9), which is derived from the normal vectors, is a measure of the flatness of the surface.

When the normal plane rotates, maximum values of κ are obtained, namely k_1 and k_2; these are called *principal curvatures*, and the corresponding curves of intersection are called principal lines of curvature. The principal curvatures k_1 and k_2 have a product and an arithmetic mean known as the *Gaussian curvature K* and the *mean curvature H*, respectively:

$$k_1 + k_2 = 2H \qquad (10a)$$

$$k_1k_2 = K \qquad (10b)$$

A spherical or ellipsoidal shell has positive Gaussian curvature (i.e., it is "convex"), a hyperbolic sheet has negative Gaussian curvature (i.e., it is "concave"), and a cylinder, cone, or flat surface has zero Gaussian curvature.

3.2 Pseudospheres, Monkey Saddles, and Infinite Periodic Minimal Surfaces. Consider surfaces with *constant* curvatures that can be embedded in 3D space. Such a surface with constant *positive* curvature is well-known to be a sphere. However, such surfaces with constant *negative* curvature do not include any shapes as simple as a sphere. In fact, there is no way of embedding the *entire* hyperbolic plane in 3D space as a surface of constant negative curvature. However, there are certain surfaces that will serve for a portion of the hyperbolic plane of finite area. The simplest example of such a surface is the socalled *pseudosphere*, which is the horn-shaped surface (Figure 6a) described by the parametric equations where $u \geq 0$:

$$x = \text{sech}\, u \cos v \qquad (11a)$$

$$y = \text{sech}\, u \sin v \qquad (11b)$$

$$z = u - \tanh u \qquad (11c)$$

However, because of the singularity (cuspidal edge) of the pseudosphere where $u = 0$, the pseudosphere, unlike its positive curvature counterpart (namely, the sphere), is of no use as a surface in which to embed networks of atoms to describe chemical structures or other chemical phenomena. In particular, the singularity in the pseudosphere is incompatible with any use to describe periodic chemical structures.

Surfaces of negative curvature that, unlike the pseudosphere, are useful for describing certain chemical structures, are known as infinite periodic minimal surfaces (IPMSs).[12,13] In this context, minimal surfaces are surfaces where the mean curvature H at each point is zero so that $k_1 = -k_2$ by eq 10a and $K \leq 0$ by eq 10b. Thus, all minimal surfaces are negative curvature surfaces constructed from hyperbolic planes. Minimal surfaces are saddle-shaped everywhere except at certain "flat points", which are higher order saddles. The simplest example of a (nonperiodic) minimal surface excluding the trivial case of the plane is defined by the following cubic equation:

$$F(x,y) = z = x(x^2 - 3y^2) \qquad (12)$$

This surface (Figure 6b) is called the *monkey saddle*,[14] because it has three depressions (namely, two for the monkey's legs and one for his tail). The *average* curvature of the monkey saddle vanishes at every point so that at every point its "concavity" is equal to its "convexity." However, the only flat point of the monkey saddle is the single point at its origin (Figure 6b).

It is not possible to construct an infinite surface with a *constant* negative Gaussian curvature as already noted. However, H. A. Schwarz found before 1865 that patches of *varying* negative curvature and constant zero mean curvature could be smoothly joined to give an infinite surface with zero mean curvature that is periodic in all three directions. Such surfaces are called IPMSs. About five different types of IPMSs were known by 1880,[15] and the

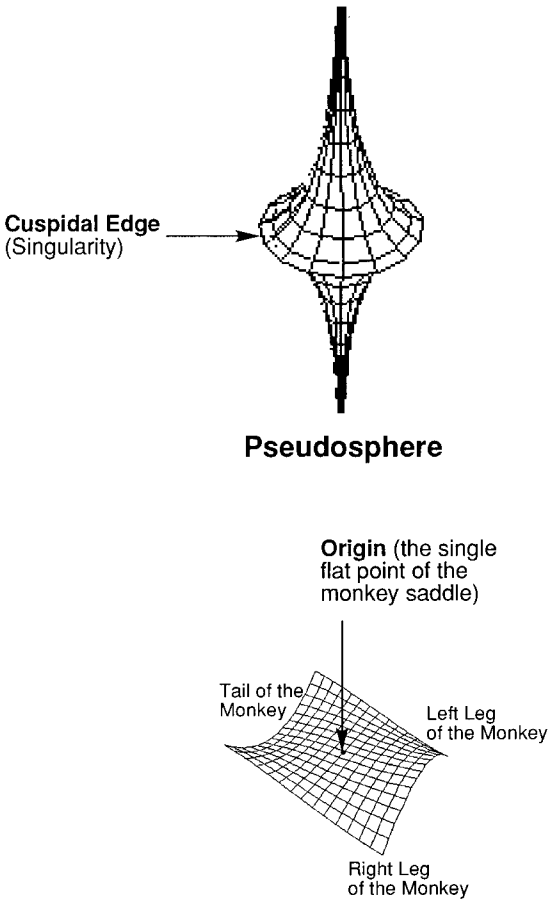

Figure 6. (a) The pseudosphere showing its cuspidal edge. (b) The monkey saddle showing its single flat point in the center.

Table 2. Polyhedral Unit Cells for the Five Classical Minimal Surfaces

surface	genus	polyhedron	symmetry	number of edges
P	3	octahedron	O_h	6 out of 12
D	3	tetrahedron	T_d	4 out of 6
T	3	cube	O_h	8 out of 12
CLP	3	trigonal prism	D_{3h}	
H	3	triangle	D_{3h}	3 out of 3

number of known distinct IPMSs is now >50.[16] The original five IPMSs have been given the designations P, D, T, H, and CLP (Table 2).[15] These IPMSs can be constructed using monkey saddles (Figure 6b) as basic building blocks so that the single flat point of each monkey saddle is located at a vertex of the polyhedral unit cell.

The IPMSs just described cannot be defined by analytic functions in the usual Cartesian space of three dimensions but instead require elliptic or hyperelliptic integrals, which must be solved numerically. The finite surface element building block that is repeated periodically throughout space in an IPMS plays a role analogous to the unit cell in a crystal structure. Hyde and collaborators[2,1718] have exploited this analogy to describe crystal structures using IPMSs.

The description of IPMSs using elliptic or hyperelliptic integrals is facilitated by the fact that minimal surfaces are the only surfaces other than the sphere whose spherical representation is conformal. This means that every complex

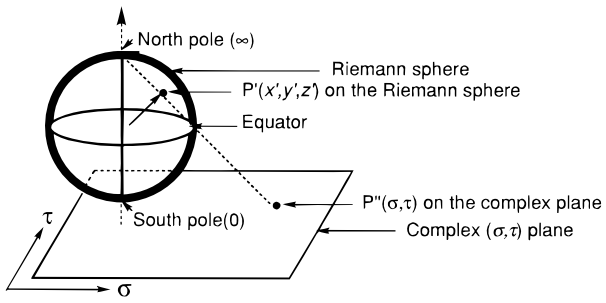

Figure 7. Riemann sphere and the projection of a point $P'(x',y',z')$ on the Riemann sphere to a point $P''(\sigma,\tau)$ in the complex plane.

analytic function can be used to describe a minimal surface. To generate such a description, each point $P(x,y,z)$ of the surface is mapped onto a point $P'(x',y',z')$ on the unit sphere given by:

$$P'(x',y',z') = \frac{\left(\frac{dF}{dx'}, \frac{dF}{dy'}, \frac{dF}{dz}\right)}{\sqrt{\left(\frac{dF}{dx}\right)^2 + \left(\frac{dF}{dy}\right)^2 + \left(\frac{dF}{dz}\right)^2}} \quad (13)$$

The same sphere, taken as a special unit sphere called the *Riemann sphere*, can also be used to represent the complex numbers $\omega = \sigma + i\tau$ by points on the (σ,τ) complex plane (Figure 7). The complex plane can correspond to the equatorial plane of the Riemann sphere (Figure 7) in which the north pole is ∞ and the south pole is 0; the $0-\infty$ axis is called the *polar axis*.[19] In this way, the point $P'(x',y',z')$ on the Riemann sphere can be projected to the point $P''(\sigma,\tau)$ on the complex plane (Figure 7). Weierstrass showed in the 19th century that the Cartesian coordinates of a point $P(x,y,z)$ on an IPMS are related to the coordinates $P''(\sigma,\tau)$ on the complex plane by the following integrals:

$$x = \mathrm{Re} \int (1 - \omega^2) R(\omega)\, d\omega \quad (14a)$$

$$y = -\mathrm{Im} \int (1 - \omega^2) R(\omega)\, d\omega \quad (14b)$$

$$z = \mathrm{Re} \int 2\omega R(\omega)\, d\omega \quad (14c)$$

in which Re and Im denote the real and imaginary parts of the complex integral and $\omega = \sigma + i\tau$, as already stated.

The Weierstrass function $R(\omega)$ determines the intrinsic parameters of the surface. For example, the Gaussian curvature is related to $R(\omega)$ by the following equation:

$$K = \frac{-4}{(1 + |\omega|^2)^4 |R(\omega)|^2} \quad (15)$$

The general form of the Weierstrass function can be expressed as follows:

$$R(\omega) = \frac{1}{(F(\omega))^{1/b}} = \frac{1}{\prod_{i=1}^{k} (\omega - \omega_i)^{1/b}} \quad (16)$$

in which $k = 8$ and $b = 2$ for the IPMSs of greatest interest. The integrals in eq 14 are hyperelliptic integrals if $b = 2$ and the degree of the polynomial $F(\omega)$ in eq 16 is greater than four. The values of the roots ω_i of the polynomial $F(\omega)$ correspond to the locations of the singular flat points of the monkey saddles (Figure 6b) making up the IPMS.

Table 2 lists the five classical IPMSs. Among these five IPMSs, two of them, namely the D and P surfaces, have the same Weierstrass function, namely:

$$R(\omega) = \frac{1}{\sqrt{1 - 14\omega^4 + \omega^8}} \tag{17}$$

The integrals (eq 14) determining the coordinates of these surfaces are hyperelliptic integrals because the degree of the polynomial in ω under the radical sign in eq 17 is greater than four. Furthermore, the locations of the eight roots of the polynomial in the denominator of eq 17 correspond to the vertices of a cube inscribed in the Riemann sphere in accord with the cubic symmetry of the unit cell of the D and P surfaces. Polynomials of this type, which vanish at the vertices of a regular polyhedron inscribed in the Riemann sphere, are called *polyhedral polynomials* and have been studied for the regular polyhedra, particularly in connection with the solution of the general quintic equation using elliptic functions.[20−22]

The transformation defined by the following coordinates is used to relate IPMSs that have the same Weierstrass function $R(\omega)$:

$$x = \mathrm{Re} \int e^{i\theta}(1 - \omega^2)R(\omega)\, \mathrm{d}\omega \tag{18a}$$

$$y = -\mathrm{Im} \int e^{i\theta}(1 + \omega^2)R(\omega)\, \mathrm{d}\omega \tag{18b}$$

$$z = \mathrm{Re} \int e^{i\theta}\, 2\omega\, R(\omega)\, \mathrm{d}\omega \tag{18c}$$

This transformation is called a *Bonnet transformation* and the angle θ is called the *association parameter*. Surfaces related by a Bonnet transformation are called *associate surfaces*. All associate surfaces have the same metrics so that lengths are preserved during any Bonnet transformation. Thus, a Bonnet transformation only bends the surface without stretching. The P and D surfaces are special cases of associate surfaces because the Bonnet transformations converting either the P to the D surface or vice versa both have $\theta = \pi/2$. Surfaces related by Bonnet transformations having $\theta = \pi/2$ are called *adjoint* surfaces.

3.3 The Genus of Infinite Periodic Minimal Surfaces: A Plumber's Nightmare. An important property of a surface is its genus where the genus of a surface corresponds to the number of holes that must be drilled through a plastic sphere to make a surface homeomorphic to the surface in question. Thus, the genus of a sphere itself is zero and the genus of a torus is one. Surfaces of higher genus have been called pretzels because of their resemblance to pretzels. A surface of genus g may also be considered to be homeomorphic to a sphere with g handles. This situation leads to the facetious observation that a topologist is a mathematician who cannot tell the difference between a doughnut (torus) and a coffee cup (with a handle) because both have a genus of one.

The nature of the IPMSs provides a clue to determine the lowest genus possible for their unit cells. Thus, the surface enclosed in a primitive unit cell of an IPMS is a 3D fundamental region. If the opposite faces of this cell are identified two by two, similar to Figure 5, a toroidal surface is obtained, embedded in a space that is the hypertorus T_3. The genus of this toroidal surface is the same as the corresponding IPMS, and this genus must also be that of the toroidal surface built from the unit cell in the hyperbolic plane. The genus of an IPMS cannot be <3, because the identification of the six faces of the simplest 3D cell leads to the formation of a toroidal surface with at least three handles. The genus could also be >3, but because all of the IPMSs of interest are of genus 3, this paper will consider only IPMSs of genus 3.

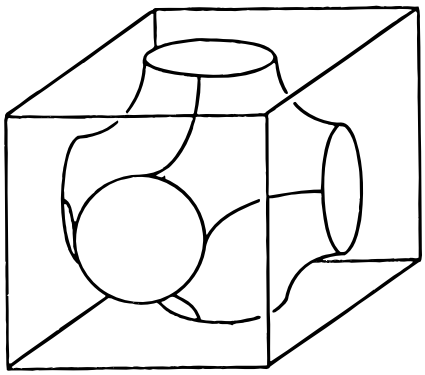

Octahedral Junction of Six Pipes
(The "Plumber's Nightmare")

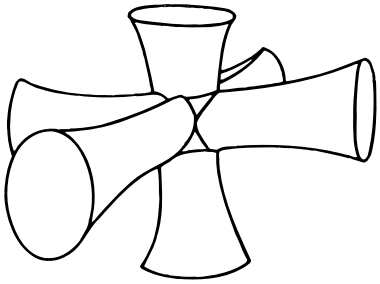

Three Hyperboloids with Axes
Meeting at Right Angles

Figure 8. Two descriptions of the unit cell of the P surface. (a) A "plumber's nightmare" intersection of six pipes coming through the faces of a cube to meet at an octahedral junction. (b) Three hyperboloids with axes meeting at right angles.

The unit cell of the P surface is depicted in two different ways in Figure 8. Thus, it can be viewed as an octahedral junction of six pipes or tubes that has been called a "plumber's nightmare" (Figure 8a) or, equivalently, as three hyperboloids whose axes meet at right angles (Figure 8b); the latter view emphasizes the negative Gaussian curvature of the P surface. Connecting the open pipes emerging from each of the three pairs of cis (i.e., adjacent) faces of the plumber's nightmare (Figure 8a), thereby identifying these three pairs of adjacent faces, generates a closed surface that is homeomorphic to a sphere with three handles, thereby indicating that this surface has genus 3.

3.4. Generalization of Euler's Theorem to Infinite Periodic Minimal Surfaces and Other Genus 3 Surfaces. The standard version of Euler's theorem relating the numbers of vertexes (v), edges (e), and faces (f) is:

$$v - e + f = 2 \tag{19}$$

This theorem applies to polyhedra that can be embedded in

a sphere or a surface homeomorphic to a sphere and thus have genus zero. For example, this theorem thus applies to all five regular polyhedra depicted in Figure 2 (see Table 1).

Euler's theorem can be generalized to polyhedra (or other polygonal networks) embedded in a surface of genus g by using eq 20:

$$v - e + f = 2(1 - g) \tag{20}$$

Note that if $g = 0$ (i.e., for polyhedra homeomorphic to a sphere), eq 20 reduces to eq 19. Also for regular tessellations on a surface of genus 3, such as the simpler IPMSs already discussed, eq 20 for $g = 3$ becomes

$$v - e + f = -4 \tag{21}$$

Equation 21 can be used to determine the number of polygons of different sizes in the unit cells of regular tessellations on hyperbolic surfaces of genus 3, including the unit cells of the IPMSs already discussed. First, however, let us see how the standard version of Euler's theorem for polyhedra of genus zero (eq 19) can be used to derive the number of faces and vertex degrees of the five regular polyhedra (Table 1 and Figure 2).

First, apply eq 19 to a regular polyhedron with all degree 3 vertices so that:

$$2e = 3v \tag{22}$$

because each edge connects exactly two vertices and each vertex is an endpoint of exactly three edges. In addition, each edge is shared by exactly two faces leading to the relationship:

$$\sum_n f_n = 2e \tag{23}$$

Now consider regular polyhedra containing only triangular, square, or pentagonal faces so that:

$$2e = 3v = 3f_3 + 4f_4 + 5f_5 \tag{24}$$

Substituting this into Euler's equation (eq 19) gives:

$$\sum (6 - k)f_k = 12 \tag{25}$$

Setting in turn $f_4 = f_5 = f_{>5} = 0$, $f_3 = f_5 = f_{>5} = 0$, and $f_3 = f_4 = f_{>5} = 0$, gives the solutions $f_3 = 4$, $f_4 = 6$, and $f_5 = 12$ for the regular tetrahedron, the cube, and the regular dodecahedron, respectively. Using a similar approach for regular polyhedra with all degree 4 vertexes gives the following equation:

$$2e = 4v = 3f_3 + 4f_4 + 5f_5 \tag{26}$$

which, when substituted into Euler's equation (eq 19) gives:

$$\sum (4 - k)f_k = 8 \tag{27}$$

Setting $f_4 = f_5 = f_{>5} = 0$ gives $f_3 = 8$, corresponding to the regular octahedron; no other regular polyhedra can be generated from eq 27. Finally, a similar approach for regular polyhedra with all degree 5 vertexes leads to:

$$2e = 5v = 3f_3 + 4f_4 + 5f_5 \Rightarrow (10-3k)f_k = 20 \tag{28}$$

Setting $f_4 = f_5 = f_{>5} = 0$ gives $f_3 = 20$, corresponding to the regular icosahedron; no other regular polyhedra can be generated from eq 28.

Now let us apply a similar approach to genus 3 surfaces arising from regular hyperbolic tessellations because this can provide some insight into tessellations of the IPMSs. First consider degree 3 hyperbolic tessellations; that is, those of the type $\{p,3\}$ on genus 3 surfaces. In this case, eq 22 for the degree 3 tessellation is substituted into the Euler's equation for the genus 3 surface (eq 21) to give:

$$\sum (6 - k)f_k = -24 \tag{29}$$

Setting $f_{\neq 7} = 0$ gives $f_7 = 24$ and setting $f_{\neq 8} = 0$ gives $f_8 = 12$, corresponding to the unit cells of the $\{7,3\}$ and $\{8,3\}$ tessellations, respectively, when embedded into a genus 3 IPMS such as the P surface.

The 24 heptagons in the unit cell of the $\{7,3\}$ tessellation can be seen in Figure 3. Thus, a "central" heptagon (heptagon 1) is surrounded by seven additional heptagons (heptagons 2−8). An "outer group" of an additional seven heptagons (heptagons 9−15) is visible, whereas heptagons 16−22 are generated by joining their halves by identifying the 14 outer edges as indicated by the letters A−G. This procedure brings together the remaining two heptagons by joining seven of the pieces that are the 14 "points" of the open network in Figure 3 not allocated to heptagons (heptagons 1−15) or heptagon halves (heptagons 16−22).

Now consider degree 4 hyperbolic tessellations; that is, those of the type $\{p,4\}$ on genus 3 surfaces. In this case, eq 26 is substituted in eq 21 to give:

$$\sum (4 - k)f_k = -16 \tag{30}$$

Setting $f_{\neq 5} = 0$ gives $f_5 = 16$ and setting $f_{\neq 6} = 0$ gives $f_6 = 8$, corresponding to the unit cells of the $\{5,4\}$ and $\{6,4\}$ tessellations, respectively. These tessellations are depicted in Figure 4.

4. CHEMICAL APPLICATIONS

4.1 Low-Density Polymeric Carbon Allotropes. One of the most exciting developments in chemistry in recent years has been the discovery of new allotropes of carbon exhibiting finite molecular cage structures rather than the infinite polymeric structures found in diamond and graphite. The first such molecular carbon cage was C_{60}, which was shown to have a truncated icosahedral structure with icosahedral symmetry resembling a soccer ball. Subsequent studies led to the discovery of other molecular C_n cages (e.g., n = 70, 76, 78, 80, 82, 84, and 90) exhibiting other polyhedral structures, albeit with much lower symmetry.[23] Such molecular carbon cages are now called *fullerenes* in recognition of their resemblance to the architectural creations of R. Buckminster Fuller.

The structures of the fullerenes, like that of graphite, are based on networks of trigonal sp^2 carbon atoms in which all vertexes have degree 3. The graphite structure, in which all of the carbon rings are hexagons, is a flat surface with zero curvature. The surfaces of the fullerene cages may be regarded as closed surfaces of positive curvature and genus zero. The original form of Euler's equation, namely eq 19, applies to fullerene structures. The carbon rings on the

Table 3. Types of Carbon Allotropes Based on Networks of Polygons of sp^2-hyBridized Carbon Atoms

allotrope	curvature	dimensionality	extent	ring sizes	density, g/cm^3
fullerenes	positive	3	finite	6,5	1.71 (C_{60})
graphite	zero	2	infinite	6	2.22
schwarzites	negative	3	infinite	6,7,8	1.2 (D168)

Table 4. Proposed Schwarzite Structures

	unit cell			
allotrope	density, g/cm^3	atom	faces	literature
schwarzite D168	1.2−1.3	168	56 f_6 + 24 f_7	27
schwarzite P192	1.16 g/cm^3	192	80 f_6 + 12 f_8	26
schwarzite P216	1.02 g/cm^3	216	80 f_6 + 24 f_7	25

positive curvature surfaces of such fullerene cages include 12 pentagons in addition to an indeterminate number of hexagons. This is in accord with eq 25, which is derived from Euler's equation (eq 19) and the fact that all carbon vertexes in fullerenes are of degree 3 (e.g., eq 22). The carbon pentagons in fullerene structures may be regarded as the source of their positive curvature.

This simple analysis of the structures of graphite and fullerenes suggests a fourth form of elemental carbon based on networks of trigonal sp^2 carbon atoms decorating surfaces of negative rather than positive curvature. Suitable negative curvature surfaces of interest are the IPMSs already discussed and are expected to lead to polymeric carbon allotropes having unusually low density, because of the porous nature of such surfaces. Because the relevant negative curvature surfaces were first studied in detail by the mathematician H. A. Schwarz in 1880,[24] the trivial name *schwarzite* has been suggested for this still unknown form of carbon.[25] The carbon rings on the negative curvature surfaces of schwarzite structures are expected to include heptagons and/or octagons in addition to an indeterminate number of hexagons. The carbon heptagons and octagons introduce negative curvature into the schwarzite surfaces. The relationships between the fullerenes, schwarzites, and graphite are summarized in Table 3.

Mackay and Terrones appear to have been the first to recognize the possibility of negative curvature allotropes of carbon and in 1991[26] they proposed the P192 schwarzite structure with a unit cell of 192 carbon atoms in a simple cubic structure based on the IPMS called the P surface. Their proposed schwarzite structure was quickly followed by the 216 atom unit cell P216 and D216 schwarzite structures of Lenosky, Gonze, Teter, and Elser[25] based on the P and D surfaces, respectively, and the 168 atom unit cell D168 schwarzite structure of Vanderbilt and Tersoff,[27] also based on the D surface. Subsequently, schwarzite structures with only one type of carbon atom in a 24-atom unit cell were studied by O'Keeffe, Adams, and Sankey.[28] The relationship between some of these proposed schwarzite structures is summarized in Table 4.

The unit cells in the proposed schwarzite structures are based on IPMSs of genus 3 and can be derived from the {7,3} and {8,3} tessellations already discussed by "diluting" the heptagons and octagons of the {7,3} and {8,3} tessellations, respectively, by hexagons so that no pair of heptagons or octagons shares an edge. This dilution process is analogous to the construction of the truncated icosahedral

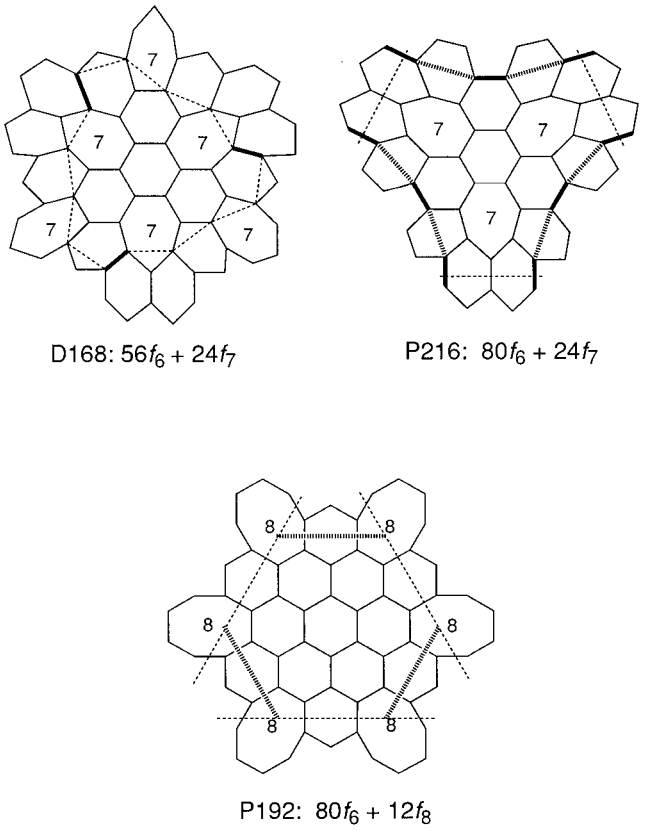

Figure 9. The arrangement of carbon polygons in octants of the unit cells in the schwarzite structures D168, P216, and P192 (Table 4). Boundaries between adjacent octants are indicated by dashed lines and boundaries with the three "pipes" meeting at each octant are indicated by hashed or solid lines.

C_{60} fullerene structure, where no pair of the 12 pentagonal faces shares an edge. Despite this dilution process, note that the schwarzite structures based on the {7,3} tessellation, namely D168 and P216, both have 24 heptagons in their unit cells, and the schwarzite structure based on the {8,3} tessellation, namely P192, has 12 octagons in its unit cell as required by eq 25 already discussed (Table 4).

Further details of the topology of these schwarzite structures can be described by the network of carbon rings in an octant of the "plumber's nightmare" representing the unit cell of the proposed structure, where an octant of the plumber's nightmare corresponds to a vertex of the cube in which the plumber's nightmare is inscribed in Figure 8a or to a (triangular) face of the octahedron dual to that cube. The networks of carbon hexagons, heptagons, and octagons in such a unit cell octant for each of the three schwarzite structures in Table 4 are depicted in Figure 9 where the boundaries with adjacent octants are represented by dashed lines and the boundaries with the "pipes" are represented by bold or hashed lines. Note that the numbers of entire polygons of each type present in an octant of each schwarzite structure in Figure 9 corresponds to $^1/_8$ of the numbers of the corresponding polygons in the unit cell listed in Table 4. For example, the octant of the unit cell of the D168 structure in Figure 9 can be seen to have three entire heptagons and seven entire hexagons corresponding to $^1/_8$ of the 24 heptagons and 56 hexagons in its unit cell.

4.2 Bilayers in Liquid Crystal and Micellar Structures. Sadoc and Charvolin[5] developed a topological theory of

bilayers in liquid crystal and micellar structures and have applied their ideas to crystals of surfaces or films formed by amphiphilic molecules in the presence of water.[29] Their theory is based on the idea that the local interactions of such molecules and packing constraints lead to strain, which they call *geometric frustration*. This frustration is relaxed if the film is transferred into 3D space with positive Gaussian curvature modeled by the hypersphere, S_3. Therein, the film built by the interfaces is supported by the spherical torus, T_2, a surface of genus 1 that separates S_3 into two identical subspaces. Because the spherical torus, T_2, can be generated by identifying opposite boundaries of a flat plane (Figure 5), its regular tessellations correspond to those on flat surfaces and thus include the {4,4} tessellation (Figure 1).

To use this model for real films formed by amphiphilic molecules, it is necessary to relate the curved hypersphere S_3 in this model to actual flat Euclidean space R_3. The curvature of S_3 can be suppressed by the introduction of so-called Volterra defects of rotation, or disclinations, around the symmetry axes of the relaxed structure in S_3 as described in detail elsewhere.[10,29] The main consequence of this procedure is that the spherical torus, which admits the {4,4} tessellation (Figure 5), is transformed into an IPMS of negative curvature admitting a {6,4} tessellation (Figure 4). However, such an IPMS cannot be associated with a surface of constant negative Gaussian curvature because the hyperbolic plane cannot be embedded in R_3. The need to understand the relationship between IPMSs and the hyperbolic plane has led to a study of 2D crystallography in the hyperbolic plane with particular emphasis on the properties of the {6,4} tessellation on such surfaces.[10] These are analogous to the relationship between a flat plane and a cylinder or torus (e.g., Figure 5).

5. SUMMARY

Regular tessellations of polygons are not only possible for flat planes (e.g., the {4,4}, {6,3}, and {3,6} tessellations in Figure 1) and the sphere (e.g., the {3,3}, {4,3}, {3,4}, {5,3}, and {3,5} tessellations corresponding to the regular polyhedra in Figure 2) but also for surfaces of negative Gaussian curvature, of which the {7,3}, {8,3}, and {6,4} tessellations (Figures 3 and 4) are of greatest actual or potential chemical interest. However, it is not possible to construct an infinite surface with a *constant* negative Gaussian curvature to accommodate such tessellations because the pseudosphere (Figure 6a), the negative curvature "analogue" of the sphere, has an inconvenient cuspidal edge singularity that prevents it from being used to describe periodic chemical structures. However, patches of *varying* negative curvature and constant zero mean curvature can be smoothly joined to give an IPMS that has zero mean curvature and that is periodic in all three directions. The unit cell of an IPMS has genus 3 so that the unit cells of the {7,3}, {8,3}, and {6,4} tessellations on such an IPMS can be shown by a generalization of Euler's theorem to contain 24 heptagons, 12 octagons, and 8 hexagons, respectively. The {7,3} and {8,3} tessellations on suitable IPMSs can be used as a basis for possible structures of low-density polymeric carbon allotropes. The {6,4} tessellation on similar IPMSs is the basis of a theory by Sadoc and Charvolin to describe the properties of bilayers in liquid crystal and micellar structures.

REFERENCES AND NOTES

(1) King, R. B. Chemical Applications of Topology and Group Theory. 29. Low-Density Polymeric Carbon Allotropes Based on Negative Curvature Structures. *J. Phys. Chem*., **1996**, *100*, 15096−15104.

(2) Hyde, S. T. Hyperbolic Surfaces in the Solid State and the Structure of ZSM Zeolites. *Acta Chem. Scand*. **1991**, *45*, 860−863.

(3) Blum, Z.; Hyde, S. T.; Ninham, B. W. Adsorption in Zeolites, Dispersion Self-Energy, and Gaussian Curvature. *J. Phys. Chem*. **1993**, *97*, 661−665.

(4) Hyde, S. T.; Andersson, S. The Martensite Transition and Differential Geometry, *Z. Kristallogr*. **1986**, *174*, 225−236.

(5) Sadoc, J. F.; Charvolin, J. Frustration in Bilayers and Topologies of Liquid Crystals of Amphiphilic Molecules. *J. Physique* **1986**, *47*, 683−691.

(6) Grünbaum, B.; Shephard, G. C. *Tilings and Patterns: An Introduction*; Freeman: New York, 1989.

(7) Coxeter, H. S. M.; Moser, W. O. J. *Generators and Relations for Discrete Groups*; Springer-Verlag: Berlin, 1972.

(8) (a) Klein, F. Über die Transformation siebenter Ordnung der elliptische Funktionen. *Math. Ann.* **1879**, *14*, 428−471; (b) Klein, F. *Gesammelte Mathematische Abhandlungen*; Springer-Verlag: Berlin, 1923; Vol. 3, pp 90−136.

(9) Coxeter, H. S. M. The Abstract Groups $G^{m,n,p}$. *Trans. Am. Math. Soc*., **1939**, *45*, 73−150.

(10) Sadoc, J. F.; Charvolin, J. Infinite Periodic Minimal Surfaces and their Cyrstallography in the Hyperbolic Plane. *Acta Crystallogr*. **1989**, *A45*, 10−20.

(11) Goetz, A. *Introduction to Differential Geometry*; Addison-Wesley: Reading, MA, 1970.

(12) Hyde, S.; Andersson, S.; Larsson, K.; Blum, Z.; Landth, T.; Lidin, S.; Ninham, B. W. *The Language of Shape*; Elsevier: Amsterdam, 1997.

(13) Andersson, S.; Hyde, S. T.; Larsson, K.; Lidin, S. Minimal Surfaces and Structures: From Inorganic and Metal Crystals to Cell Membranes and Biopolymers. *Chem. Rev*. **1988**, *88*, 221−242.

(14) Hilbert, D.; Cohn-Vossen, S. *Geometry and the Imagination*; Chelsea Publishing: New York, 1952; pp 183−204.

(15) Neovius, E. R. *Bestimmung Zweier Spezieller Periodische Minimalflächen*; J. C. Frenkel & Sohn: Helsinki, 1883.

(16) Fischer, W.; Koch, E. New Surface Patches of Minimal Balance Surfaces. I. Branched Catenoids. *Acta Crystallogr*. **1989**, *A45*, 166−169; Fischer, W.; Koch, E. II. Multiple Catenoids. *Acta Crystallogr*. **1989**, *A45*, 169−174; Fischer, W.; Koch, E. III. Infinite Strips. *Acta Crystallogr*. **1989**, *A45*, 485−490; Fischer, W.; Koch, E. IV. Catenoids with Spout-Like Attachments. *Acta Crystallogr*. **1989**, *A45*, 558−563; Fischer, W.; Koch, E. Genera of Minimal Balance Surfaces. *Acta Crystallogr*. **1989**, *A45*, 726−732.

(17) Andersson, S.; Hyde, S. T.; von Schnering, H. G. The Intrinsic Curvature of Solids. *Z. Kristallograph*. **1984**, *168*, 1−17.

(18) Hyde, S. T. A Topological Characterization of Chemical Structures. *Z. Kristallograph*. **1987**, *179*, 53−65.

(19) Klein, F. *Vorlesungen über das Ikosaeder*; Teubner: Leipzig, 1884; Part I, Chapter II.

(20) Dickson, L. E. *Modern Algebraic Theories*; Sanborn: Chicago, 1930; Chapter XIII.

(21) King, R. B.; Canfield, E. R. Icosahedral Symmetry and the Quintic Equation. *Comput. Math. Appl*. **1992**, *24(3)*, 13−28.

(22) King, R. B. *Beyond the Quartic Equation*; Birkhäuser: Boston, 1996.

(23) Diederich, F.; Whetten, R. L., Beyond C_{60}: The Higher Fullerenes. *Acc. Chem. Res*. **1992**, *25*, 119−126.

(24) Schwarz, H. A. *Gesammelte Mathematische Abhandlungen*; Springer: Berlin, 1890.

(25) Lenosky, T.; Gonze, X.; Teter, M.; Elser, V. Energetics of Negatively Curved Graphitic Carbon. *Nature* **1992**, *355*, 333−335.

(26) Mackay, A. L.; Terrones, H. Diamond from Graphite. *Nature* **1991**, *352*, 762.

(27) Vanderbilt, D.; Tersoff, J. Negative-curvature Fullerene Analogue of C_{60}. *Phys. Rev. Lett*. **1992**, *68*, 511−513.

(28) O'Keeffe, M.; Adams, G. B.; Sankey, O. F. Predicted New Low Energy Forms of Carbon. *Phys. Rev. Lett*. **1992**, *68*, 2325−2328.

(29) Charvolin, J.; Sadoc, J. F. Periodic Systems of Frustrated Fluid Films and "Bicontinuous" Cubic Structures in Local Crystals. *J. Phys. (Paris)* **1987**, *48*, 1559−1569.

CI970063+